Available online at www.sciencedirect.com
SCIENCE DIRECT®
ELSEVIER
International Journal of Thermal Sciences 42 (2003) 23–31
International Journal of Thermal Sciences
www.elsevier.com/locate/ijts

Flow and heat transfer on a stretching surface in a rotating fluid with a magnetic field

H.S. Takhar [a,*], A.J. Chamkha [b], G. Nath [c]

[a] *Department of Engineering, Manchester Metropolitan University, Manchester, M1 5GD, UK*
[b] *Department of Mechanical Engineering, Kuwait University, P.O. Box 5969, Safat, Kuwait*
[c] *Department of Mathematics, Indian Institute of Science, Bangalore 560012, India*

Received 18 April 2001; accepted 22 January 2002

Abstract

An analysis has been developed in order to study the flow and heat transfer on a stretching surface in a rotating fluid, in the presence of a magnetic field. The partial differential equations governing the non-similar flow have been solved numerically by using the implicit finite difference and the difference-differential methods. The magnetic field increases the skin friction coefficient in the x-direction, but reduces the skin friction coefficient in the y-direction and the Nusselt number also decreases. On the other hand, the skin friction coefficients in x and y directions increase, in general, with the rotation parameter, but the Nusselt number decreases. The Nusselt number also increases with the Prandtl number.

Keywords: MHD flow; Rotating fluid; Heat transfer; Stretching surface

1. Introduction

The study of flow and heat transfer in the boundary layer induced by a surface moving with a uniform or non-uniform velocity in an otherwise ambient fluid is important in several manufacturing processes in industry which include the boundary layer along material handling conveyers, the extrusion of plastic sheets, the cooling of an infinite metalic plate in a cooling bath. Glass blowing, continuous casting and spinning of fibers also involve the flow due to a stretching surface. In recent years MHD flow problems have become more important in industry. Since many metallurgical processes involve the cooling of continuous strips or filaments. By drawing them in an electrically conducting fluid in the presence of a magnetic field, the rate of cooling can be controlled. Another application is in the purification of molten metals from non-metalic inclusions by the application of a magnetic field. The flow past a moving or stretching surface in an ambient fluid differs from that of the classical Blasius problem of flow past a stationary surface. The moving surface sucks the fluid and pumps it back in the down-stream direction. Consequently, both the surface shear stress and the heat transfer are significantly enhanced. Sakiadis [1] studied the flow induced by a surface moving with a constant velocity in an ambient fluid. The corresponding heat transfer problem was considered theoretically and experimentally by Tsou et al. [2] and Erickson et al. [3] and experimentally by Griffin and Throne [4]. Crane [5] studied the same problems as in [1], but assumed that the surface velocity U varies linearly with the stream-wise distance x (i.e., $U = ax$, where a $(a > 0)$ is the velocity gradient). Gupta and Gupta [6] studied the heat and mass transfer for the boundary layer over an isothermal stretching sheet subject to blowing and suction. Subsequently Chakrabarti and Gupta [7] extended the above analysis to include the effect of a magnetic field. Carragher and Crane [8] investigated the heat transfer characteristics of a linearly stretching impermeable isothermal surface and obtained an analytical solution. Dutta et al. [9] considered the effect of the uniform flux condition on the heat transfer over a linearly stretching surface. Grubka and Bobba [10] examined the effect of the non-isothermal wall temperature, varying as a power-law with the distance x, on the heat transfer over a stretching surface. The effect of uniform suction and injection on the flow and

* Correspondence and reprints.
E-mail address: h.s.takhar@mmu.ac.uk (H.S. Takhar).

1290-0729/02/$ – see front matter
PII: S1290-0729(02)00004-2

Nomenclature

C_{fx}	skin friction coefficient in the x-direction	
C_{fy}	skin friction coefficient in the y-direction	
C_p	specific heat at constant pressure	$kJ\cdot kg^{-1}\cdot K^{-1}$
C_v	specific heat at constant volume	$kJ\cdot kg^{-1}\cdot K^{-1}$
f, g	dimensionless similarity variables	
g	acceleration due to gravity	$9.81\ m\cdot s^{-2}$
h	heat transfer coefficient	$W\cdot m^{-2}\cdot K^{-1}$
Ha	Hartmann number	
k	thermal conductivity	$W\cdot m^{-1}\cdot K^{-1}$
L	characteristic length	m
M	magnetic parameter	
Nu_x	local Nusselt number	
p	pressure	$Pa, N\cdot m^{-2}$
Pr	Prandtl number	
q	heat flux	$W\cdot m^{-2}$
Re	Reynolds number	
T	temperature	K
u, v, w	velocity components	$m\cdot s^{-1}$

Greek letters

α	thermal diffusivity	$m^2\cdot s^{-1}$
β	coefficient of thermal expansion	K^{-1}
η, ξ	transformed similarity variables	
μ	dynamic viscosity	$kg\cdot m^{-1}\cdot s^{-1}$
ν	kinematic viscosity	$m^2\cdot s^{-1}$
ρ	density	$kg\cdot m^{-3}$
λ	rotation parameter	
Ω	angular velocity	
ψ	stream function	$m^2\cdot s^{-1}$

heat transfer from a stretching sheet was analysed by Dutta [11] who also obtained an analytical solution. Chappadi and Gunnerson [12] examined the flow and mass transport on a surface which is moving with a uniform velocity in an otherwise ambient fluid. Andersson [13] studied the flow of an electrically conducting fluid on a linearly stretching surface with a magnetic field and also obtained an analytical solution of the Navier–Stokes equations. The effect of the variable thermal conductivity on the heat transfer in the stagnation-point flow towards a linearly stretching sheet was examined by Chiam [14], who obtained the solution of the governing ordinary differential equations numerically. Vajravelu and Hadjinicolaou [15] carried out an analysis for the flow and heat transfer of a viscous electrically conducting fluid over a vertical isothermal sheet which is linearly stretched in the presence of a uniform free stream. The effects of the buoyancy force and internal heat generation or absorption have been included in the analysis. The magnetic field is applied normal to the surface. The boundary layer equations given by a system of coupled non-linear ordinary differential equations were solved numerically. Kumari and Nath [16] investigated the effect of a magnetic field on the stagnation-point flow and heat transfer of a viscous electrically conducting fluid on a linearly stretching sheet. The Navier–Stokes and energy equations governing the flow and heat transfer were solved numerically. In most of the above cases the surface velocity was taken to be $U = ax$, $a > 0$ and self-similar solutions were obtained. The draw back of this model is that it gives zero velocity at the slit. Jeng et al. [17] have studied the non-similar flow over the surface which is moving with the velocity $U = U_0(1 + x/L)$, where U_0 is the velocity at $x = 0$, x is the distance along the surface, and L is the characteristic length, in an ambient fluid. Wang [18] has considered the steady flow over a linearly stretching surface ($U = ax$, $a > 0$) in a rotating fluid and has obtained a self-similar solution. Recently, Takhar and Nath [19] have extended the analysis of Wang [18] to include the effects of the magnetic field and unsteadiness and obtained a self-similar solution.

The magneto-hydrodynamics of rotating electrically-conducting fluids in the presence of a magnetic field is encountered in many important and interesting problems in geophysics and astrophysics. It can provide explanations for the observed maintenance and secular variations of the geomagnetic field [20]. It is also relevant in solar physics involved in the sunspot development, the solar cycle and the structure of rotating magnetic stars [21].

The aim of this analysis is to study the flow and heat transfer over a stretching surface in a rotating electrically-conducting fluid in the presence of a magnetic field. The parabolic partial differential equations governing the non-similar flow have been solved by using an implicit finite-difference scheme similar to that of Blottner [22]. These equations have also been solved by using the difference-differential methods [23], wherein we have to solve a system of ordinary differential equations instead of partial differential equations. The results have been compared with those of Tsou et al. [2], Erickson et al. [3], Griffin and Throne [4], and Jeng et al. [17].

Our problem can be regarded as the magnetic and rotating counter-part of the non-similar problem considered by Jeng et al. [17]. It can also be considered as the magnetic counter-part of the similar-problem considered by Wang [18] with the further difference that our problem is non-similar. Since the rotation of the fluid increases the magnitude of the secondary flow and the magnetic field decreases it, the magnetic field can play an important role in retarding the growth of the secondary flow as well as in reducing the heat transfer rate. This also justifies the study of the effect of the magnetic field on rotating flows. One possible application of the present model is in self-cooled liquid metal blankets in fusion reactors where the container is being rotated.

2. Analysis

We consider the steady motion of a viscous incompressible electrically-conducting fluid induced by the stretching of a surface in the x-direction in a rotating fluid. The surface coincides with the plane $z = 0$ and it is being stretched with velocity $U = U_0(1 + x/L)$. The fluid is rotating with a constant angular velocity Ω about the z-axis. The stretching distance x is also rotating with the fluid. The flow is three-dimensional due to the presence of the Coriolis force. Fig. 1 shows the coordinate system, where u, v and w are the velocity components in the direction of Cartesian axes x, y and z, respectively. The magnetic field B is imposed in the z-direction. Since the flow is induced by stretching the surface in the x-direction only, the velocity components, u, v, w, and the temperature T depend only on x and z. It is assumed that the magnetic Reynolds number $Re_m = \mu_0\sigma VL$ is small, where μ_0 is the magnetic permeability, σ is the electrical conductivity, and V and L are the characteristic velocity and length, respectively. Under these conditions, it is possible to neglect the induced magnetic field in comparison to the applied magnetic field. Since no applied or polarization voltage is imposed on the flow field, the electric field $\vec{E} = 0$. This corresponds to the case where no energy is added to or extracted from the fluid by electrical means. The surface is electrically insulated. Hence, the Lorenz magnetic force depends only on the magnetic field. The viscous dissipation, Joule heating, and the Hall effect are neglected. The surface temperature and the fluid temperature at the edge of the boundary layer are all constant. Under the foregoing assumptions, the boundary layer equations in the rotating frame of reference are [17–19,24] given by:

$$u_x + w_z = 0 \tag{1}$$

$$uu_x + wu_z - 2\Omega v = \nu u_{zz} - \rho^{-1}\sigma B^2 u \tag{2}$$

$$uv_x + wv_z + 2\Omega u = \nu v_{zz} - \rho^{-1}\sigma B^2 v \tag{3}$$

$$uT_x + wT_z = \alpha T_{zz} \tag{4}$$

The boundary conditions are given by:

$$\begin{aligned} &u(x,0) = U(x), \quad v(x,0) = 0 \\ &w(x,0) = 0, \quad T(x,0) = T_w, \quad x \geqslant 0 \\ &u(x,\infty) = v(x,\infty) = 0, \quad T(x,\infty) = T_\infty, \quad x \geqslant 0 \\ &u(0,z) = v(0,z) = 0, \quad T(0,z) = T_\infty, \quad z > 0 \end{aligned} \tag{5}$$

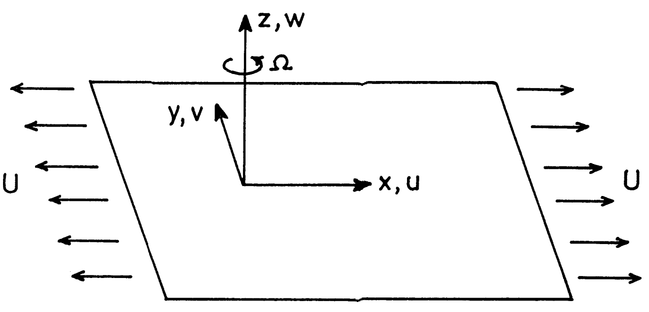

Fig. 1. Coordinate system.

Here ρ and ν are the density and kinematic viscosity of the fluid, respectively; α is the thermal diffusivity, U is the surface velocity, T_w and T_∞ are the wall temperature and temperature at the edge of the boundary layer, respectively, and the subscripts x and z denote derivatives with respect to x and z, respectively.

It is convenient to transform equations (1)–(4) from (x, z) system to $(\bar{\xi}, \eta)$ system by using the following transformations:

$$\begin{aligned} &\eta = (2\bar{\xi}\nu)^{1/2} Uz, \qquad \bar{\xi} = \int_0^x U(x)\,\mathrm{d}x \\ &U(x) = U_0(1 + x/L), \qquad \xi = x/L \\ &\psi(x,z) = (2\nu\bar{\xi})^{-1/2} f(\bar{\xi},\eta) r \\ &T(x,z) = T_\infty + (T_w - T_\infty)\theta(\bar{\xi},\eta) \\ &v(x,z) = Ug(\bar{\xi},\eta), \qquad u = \delta\psi/\delta z = Uf'(\bar{\xi},\eta) \\ &\bar{\xi} = U_0 L\xi(1+\xi/2) \\ &s_1 = (2\bar{\xi}/U)(\mathrm{d}U/\mathrm{d}\bar{\xi}) = 2\xi(1+\xi/2)(1+\xi)^{-2} \\ &\lambda = \Omega L/U_0, \qquad M = Ha^2 = \sigma B^2 L^2/\mu \\ &Re_L = U_0 L/\nu, \qquad Pr = \nu/\alpha \end{aligned} \tag{6}$$

Here $(\bar{\xi}, \eta)$ are the transformed coordinates; ψ and f are the dimensional and dimensionless stream functions, respectively; ξ is the dimensionless stream-wise distance; f' and g are the dimensionless velocity components along the x and y directions, respectively (i.e., f' and g are, respectively, the primary and secondary flow velocities); θ is the dimensionless temperature; λ is the fluid rotation parameter; M is the magnetic parameter which is the ratio of the Hartmann number to the Reynolds number; Pr is the Prandtl number; Ha is the Hartmann number; Re_L is the Reynolds number; s_1, s_2 and s_3 are functions of ξ; and prime denotes derivative with respect to η.

These transformations also convert Eqs. (1)–(4) in dimensionless form. Consequently, we find that (1) is identically satisfied and Eqs. (2)–(4) reduce to:

$$\begin{aligned} &f''' + ff'' - s_1 f'^2 + 2\lambda s_2 g - M s_2 f' \\ &\quad = s_3\xi\left(f'\partial f'/\partial\xi - f''\partial f/\partial\xi\right) \end{aligned} \tag{7}$$

$$\begin{aligned} &g'' + fg' - s_1 f'g - 2\lambda s_2 f' - M s_2 g \\ &\quad = s_3\xi\left(f'\partial g/\partial\xi - g'\partial f/\partial\xi\right) \end{aligned} \tag{8}$$

$$Pr^{-1}\theta'' + f\theta' = s_3\xi\left(f'\partial\theta/\partial\xi - \theta'\partial\theta/\partial\xi\right) \tag{9}$$

where

$$\begin{aligned} &s_2 = (2\bar{\xi}/U_0/U^2 L) = 2\xi(1+\xi/2)(1+\xi)^{-2} \\ &s_3 = (2\bar{\xi}/UL)\xi^{-1} = 2(1+\xi/2)(1+\xi)^{-1} \end{aligned} \tag{10}$$

The boundary conditions (5) can be re-written as

$$\begin{aligned} &f(\xi,0) = 0, \qquad f'(\xi,0) = 1 \\ &g(\xi,0) = 0, \qquad \theta(\xi,0) = 1 \\ &f(\xi,\infty) = g(\xi,\infty) = \theta(\xi,\infty) = 0 \end{aligned} \tag{11}$$

It may be remarked that Eqs. (7) and (9) for $\lambda = M = 0$ (in the absence of fluid rotation and magnetic field) are identical to those of Jeng et al. [17]. For $\lambda = 0$, $g(\xi, \eta) = 0$ and Eq. (8) is not required. Also, Eqs. (7) and (9) for $\xi = M = \lambda = 0$ (self-similar flow) reduce to those of Tsou et al. [2] and Erickson et al. [3] if we apply the transformations $\eta_1 = 2^{1/2}\eta$, $f_1(\eta_1) = 2^{1/2} f(\eta)$, $\theta_1(\eta_1) = \theta(\eta)$. Since Wang [18] and Takhar and Nath [19] have assumed the wall velocity $U = ax$, $a > 0$ instead of $U = U_0(1 + x/L)$, Eqs. (7)–(9) cannot directly be reduced to those of [18,19].

The quantities of physical interest are the skin friction and heat transfer coefficients. The local skin friction coefficients in the x and y directions are given by:

$$\begin{aligned} C_{fx} &= -2\mu(\partial u/\partial z)_{z=0}/\rho U_0^2 \\ &= -2^{1/2} Re_x^{-1/2}(1+\xi)^2(1+\xi/2)^{-1/2} f''(0) \\ C_{fy} &= -2\mu(\partial v/\partial z)_{z=0}/\rho U_0^2 \\ &= -2^{1/2} Re_x^{-1/2}(1+\xi)^2(1+\xi/2)^{-1/2} g'(\xi,0) \end{aligned} \tag{12}$$

Similarly, the local heat transfer coefficient in terms of the local Nusselt number can be expressed as

$$\begin{aligned} Nu_x &= -x(\partial T/\partial z)_{z=0}/(T_w - T_\infty) \\ &= -2^{1/2} Re_x^{-1/2}(1+\xi)(1+\xi/2)^{-1/2}\theta'(\xi,0) \end{aligned} \tag{13}$$

where $Re_x = U_0 x/\nu$ is the local Reynolds number; μ is the coefficient of viscosity; C_{fx} and C_{fy} are the local skin friction coefficients along x and y directions (i.e., C_{fx} and C_{fy} are the local skin coefficients for the primary and secondary flows, respectively); and Nu_x is the local Nusselt number.

3. Finite-difference method

The parabolic partial differential equations (7)–(9) along with (10) under the boundary conditions (11) have been solved by using an implicit iterative tri-diagonal finite-difference scheme similar to that of Blottner [22]. All the first-order derivatives with respect to ξ are replaced by two-point backward difference formulae

$$\partial S/\partial \xi = (S_{i,j} - S_{i-1,j})/\Delta\xi \tag{14}$$

where S denotes the dependent variable f or g or θ and i and j are the node locations along the ξ and η directions, respectively. First, the third order partial differential equation (7) is converted to a second-order partial differential equation by substituting $f' = F$. Then the second order derivatives with respect to η for F, g and θ are discretized using the three-point central difference formulae while the first-order derivatives are discretized by employing the trapezoidal rule. At each line of constant ξ, a system of algebraic equations is obtained. The nonlinear terms are evaluated at the previous iteration and the equations are solved iteratively by using the Thomas algorithm (see Blottner [22]). The same procedure is followed for the next ξ value and the equations are solved line by line until the desired ξ value is reached. A convergence criterion based on the relative difference between the current and the previous iterations is used. When this difference reaches 10^{-5}, the solution is assumed to have converged and the iterative process is terminated.

4. Difference-differential method

The partial differential equations (7)–(9) with relations (10) under the boundary conditions (11) are also solved by using the difference-differential method [23]. In this method, we have to solve a system of ordinary differential equations instead of partial differential equations. Further, these ordinary differential equations are converted to integral equations and then solved by iterative numerical quadrature. The results obtained by employing this method are nearly the same as those obtained by using the finite-difference scheme, but there is a significant reduction in the computation time.

First, we replace the derivatives with respect to ξ at $\xi = \xi_i = ih$ $(I = 0, 1, 2, \ldots)$, where h is a constant interval, by using a four-point formula of Gregory–Newton. Eqs. (7)–(9) can be replaced by the following ordinary differential equations:

$$\begin{aligned} & f_i''' + \left[f_i + s_3(i/6)(11f_i - 18f_{i-1} + 9f_{i-2} - 2f_{i-3})\right]f_i'' \\ & \quad - \left[Ms_2 + s_3(i/6)\left(11f_i' - 18f_{i-1}' + 9f_{i-2}' - 2f_{i-3}'\right)\right]f_i' \\ & \quad - s_1\left(f_i'\right)^2 + 2\lambda s_2 g_i = 0 \end{aligned} \tag{15}$$

$$\begin{aligned} & g_i'' + \left[f_i + s_3(i/6)(11f_i - 18f_{i-1} + 9f_{i-2} - 2f_{i-3})\right]g_i' \\ & \quad - \left[s_1 g_i + s_3(i/6)(11g_i - 18g_{i-1} + 9g_{i-2} - 2g_{i-3})\right]f_i' \\ & \quad - 2\lambda s_2 f_i' - Ms_2 g_i = 0 \end{aligned} \tag{16}$$

$$\begin{aligned} & Pr^{-1}\theta_i'' + \left[f_i + s_3(i/6)(11f_i - 18f_{i-1} \right. \\ & \qquad \left. + 9f_{i-2} - 2f_{i-3})\right]\theta_i' \\ & \quad - \left[s_3(i/6)(11\theta_i - 18\theta_{i-1} + 9\theta_{i-2} - 2\theta_{i-3})\right]f_i' = 0 \end{aligned} \tag{17}$$

where

$$\begin{aligned} s_1 &= s_2 = 2ih(1+ih/2)(1+ih)^{-2} \\ s_3 &= 2(1+ih/2)(1+ih)^{-1} \end{aligned} \tag{18}$$

The boundary conditions (11) can be replaced by

$$\begin{aligned} & f_i(0) = 0, \qquad f_i'(0) = 1 \\ & g_o(0) = 0, \qquad \theta_i(0) = 1 \\ & f_i'(\infty) = g_i(\infty) = \theta_I(\infty) = 0 \end{aligned} \tag{19}$$

It is possible to express the solution of (15)–(17) under conditions (19) at the ith station $\xi_i = ih$ in terms of integral equations.

$$f_i' = 1 + \int_0^\eta E(\eta) \int_0^\eta \frac{R(\eta)}{E(\eta)}\,\mathrm{d}\eta\,\mathrm{d}\eta$$

$$- \left[\int_0^\infty E(\eta) \int_0^\eta \frac{R(\eta)}{E(\eta)} \, d\eta \, d\eta \right] \frac{G(\eta)}{G(\infty)} \tag{20}$$

$$f_i = \int_0^\eta f_i' \, d\eta \tag{21}$$

$$g_i = \int_0^\eta E(\eta) \int_0^\eta \frac{H(\eta)}{E(\eta)} \, d\eta \, d\eta - \left[\int_0^\infty E(\eta) \int_0^\eta \frac{H(\eta)}{E(\eta)} \, d\eta \, d\eta \right] \frac{G(\eta)}{G(\infty)} \tag{22}$$

$$\theta_i = 1 + Pr \int_0^\eta E(\eta) \int_0^\eta \frac{P(\eta)}{E(\eta)} \, d\eta \, d\eta - Pr \left[\int_0^\infty E(\eta) \int_0^\eta \frac{P(\eta)}{E(\eta)} \, d\eta \, d\eta \right] \frac{G(\eta)}{G(\infty)} \tag{23}$$

where

$$E(\eta) = \exp\left[\int_0^\eta \{ -f_i - s_3(i/6)(11 f_i - 18 f_{i-1} + 9 f_{i-2} - 2 f_{i-3} \} \, d\eta \right] \tag{24}$$

$$R(\eta) = \left[M s_2 + s_3(i/6)\left(11 f_i' - 18 f_{i-1}' + 9 f_{i-2}' - 2 f_{i-3}'\right)\right] f_i' + s_1 \left(f_i'\right)^2 - 2\lambda s_2 g_i \tag{25}$$

$$G(\eta) = \int_0^\eta E(\eta) \, d\eta \tag{26}$$

$$H(\eta) = \left[s_1 g_i + s_3(i/6)(11 g_i - 18 g_{i-1} + 9 g_{i-2} - 2 g_{i-3}) \right] f_i' + 2\lambda s_2 f_i' + M s_2 g_i \tag{27}$$

$$P(\eta) = \left[s_3(i/6)(11\theta_i - 18\theta_{i-1} + 9\theta_{i-2} - 2\theta_{i-3}) \right] f_i' \tag{28}$$

The integral equations (20)–(23) are solved by employing an iterative numerical quadrature using the Simpson's rule. Eqs. (20)–(23) involve $f(\eta)$, $f'(\eta)$, $g(\eta)$ and $\theta(\eta)$ at locations ξ_{i-1}, ξ_{i-2}, and ξ_{i-3}. When these quantities are determined, we can get $f_i(\eta)$, $f_i'(\eta)$, $g_i(\eta)$ and $\theta_i(\eta)$ from (20)–(23). The initial functions $f_0(\eta)$, $f_0'(\eta)$, $g_0(\eta)$ and $\theta_0(\eta)$ at $\xi = M = \lambda = 0$ are the solutions of the ordinary differential equations obtained from (7)–(9) with $\xi = 0$. These ordinary differential equations at $\xi = M = \lambda = 0$ are solved by using the Runge–Kutta–Gill method [25]. Similarly, $f_1(\eta)$, $f_1'(\eta)$, $g_1(\eta)$, $\theta_1(\eta)$ and $f_2(\eta)$, $f_2'(\eta)$, $g_2(\eta)$, $\theta_2(\eta)$ at $\xi = \xi_1$ and $\xi = \xi_2$ are obtained from equations similar to (15)–(17), where the derivatives with respect to ξ are, respectively, replaced by two-point and three-point difference formulae instead of four-point formula used in (15)–(17). After these starting solutions have been obtained, we can solve (20)–(23). The convergence criterion is based on the relative difference between the current and the previous iterations. When this difference becomes 10^{-5}, the solution is assumed to have converged and the iterative process is terminated.

5. Results and discussion

Eqs. (7)–(9) with (10) under the boundary conditions (11) have been solved numerically by using the finite-difference and difference-differential methods as described earlier. In order to assess the accuracy of our methods, we have compared the velocity profile $u/U_0 = f'(\eta)$ for $\xi = 0 = M = \lambda$ with the theoretical and experimental results of Tsou et al. [2] in Fig. 2. It is in very good agreement with the theoretical values. It also agrees well with the experimental values near the wall. We have compared the local Nusselt number Nu_x for $\xi = 0$ with the theoretical values of Erickson et al. [3] and with the experimental values of Griffin and Throne [4] in Fig. 3. The results are in good agreement with the theoretical and experimental values when the wall velocity $U_0 \geqslant 8.92$ ft·s^{-1}. Further, the local skin-friction coefficient ($Re_x^{1/2} C_{fx}$) and the local Nusselt number ($2Re_x^{-1/2} Nu_x$) for $M = \lambda = 0$ (i.e., in the absence of the magnetic field and rotation of the fluid) are compared with those of Jeng et al. [17]. The results are found to be in very good agreement. The comparison is shown in Fig. 4. Also, the results obtained by both the finite-difference and the difference-differential methods are identical at least up to the third decimal place. Hence, the comparison is shown only in a few cases.

The effect of the magnetic parameter M on the local skin friction coefficients in the x and y directions, $2^{-1/2} Re_x^{1/2} C_{fx}$, $2^{-1/2} Re_x^{-1/2}$, C_{fy}, and the local Nusselt number, $2^{1/2} Re_x^{-1/2} Nu_x$, for $\lambda = 0.5$, $Pr = 0.7$, $0 \leqslant \xi \geqslant 3$, obtained by using both the finite-difference and the difference-differential methods is shown in Figs. 5–7. Since the magnetic parameter M is multiplied by ξ (see Eqs. (7), (8), (10)),

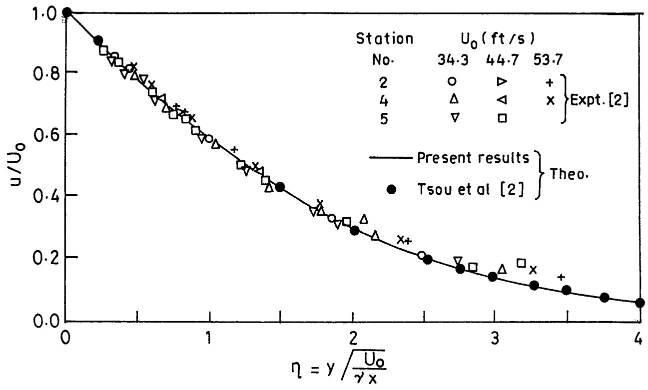

Fig. 2. Comparison of the velocity profile u/U_0 for $\xi = M = \lambda = 0$, with that of Tsou et al. [2].

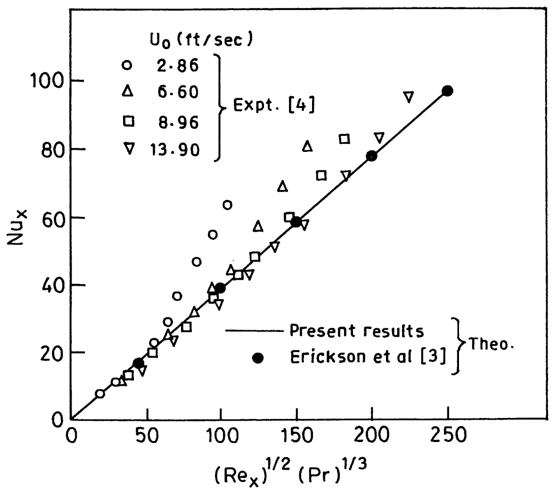

Fig. 3. Comparison of the local Nusselt number Nu_x for $\xi = M = \lambda = 0$, with that of Erickson et al. [3] and Griffin and Throne [4].

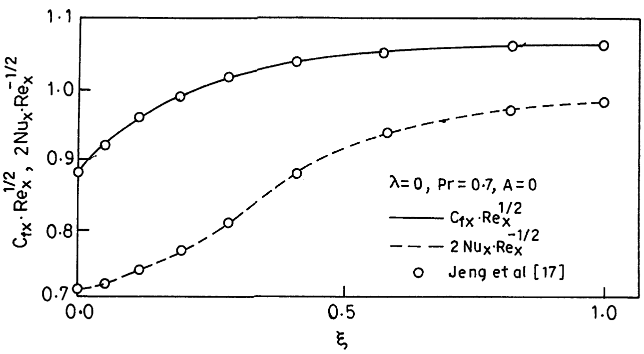

Fig. 4. Comparison of the local skin friction coefficient in x direction ($Re_x^{1/2} C_{fx}$) and the local Nusselt number ($2Re_x^{-1/2} Nu_x$) with those of Jeng et al. [17] for $\lambda = M = 0$, $Pr = 0.7$.

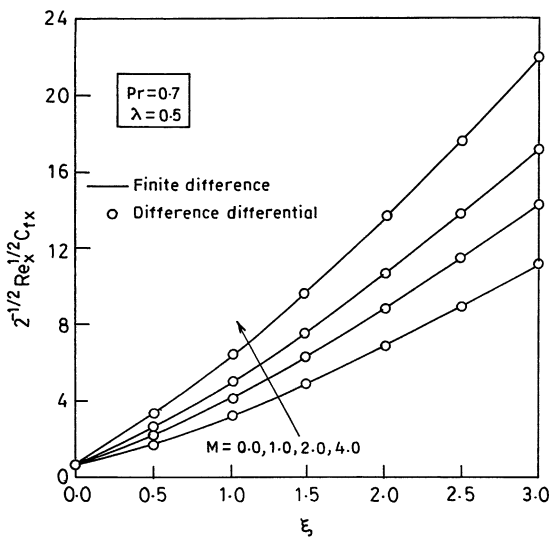

Fig. 5. Effect of the magnetic parameter M on the local skin friction coefficient in x direction ($2^{-1/2} Re_x^{1/2} C_{fx}$): — finite difference; ∘ difference differential.

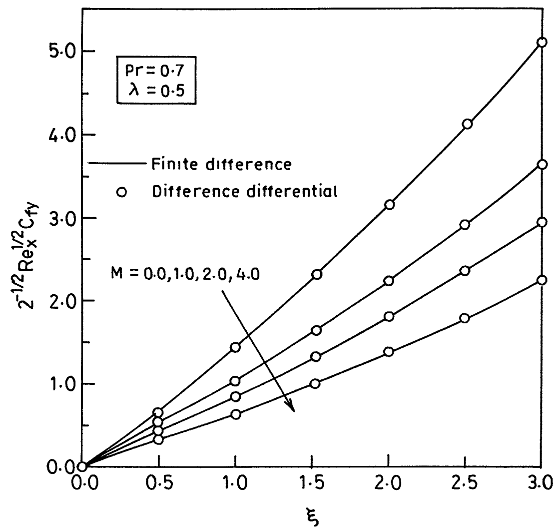

Fig. 6. Effect of the magnetic parameter M on the local skin friction coefficient in y direction ($2^{-1/2} Re_x^{1/2} C_{fy}$): — finite difference; ∘ difference differential.

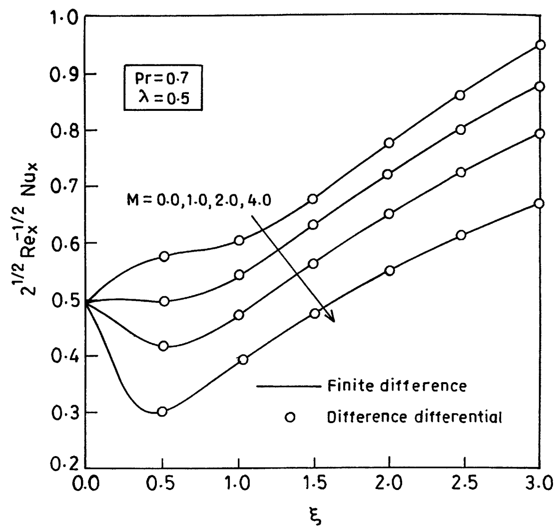

Fig. 7. Effect of the magnetic parameter M on the local Nusselt number ($2^{1/2} Re_x^{-1/2} Nu_x$): — finite difference; ∘ difference differential.

its effect vanishes at $\xi = 0$ and increases significantly with ξ. For example, for $M = 1$, $\lambda = 0.5$, $Pr = 0.7$, the skin friction coefficients in the x and y directions and the Nusselt number increase by about 833%, 525% and 74%, respectively, as ξ increases from 0.5 to 3. The reason for a comparatively weak dependence of the Nusselt number on M is that it does not occur explicitly in the energy equation (see Eq. (9)). It may be noted that in the range $0 > \xi < 0.6$, the Nusselt number decreases for $M \geqslant 2$. This trend is due to the opposing effects of the parameters in this range. For a fixed ξ, the skin friction coefficient in the x-direction increases with M, but the skin friction coefficient in the y-direction and the Nusselt number decrease. The reason for this trend is that the magnetic field has a stabilizing effect on the flow field. Hence it enhances the velocity in the x-direction $f'(\xi, \eta)$, but re-

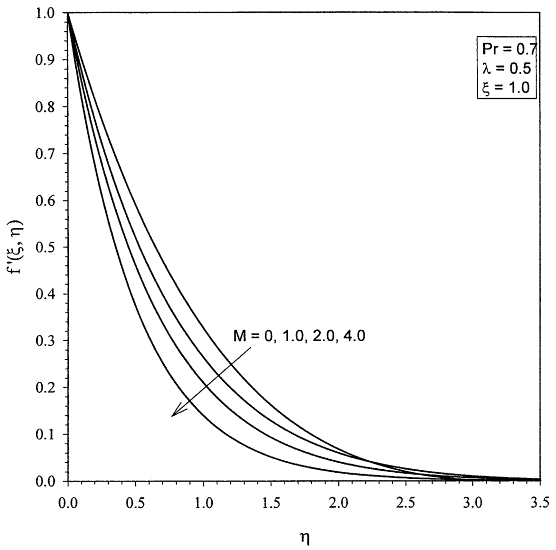

Fig. 8. Effect of the magnetic parameter M on the velocity profiles in x direction $(f'(\xi,\eta))$.

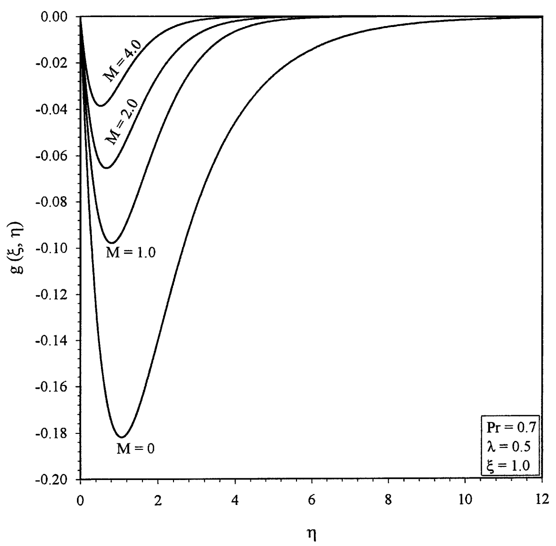

Fig. 9. Effect of the magnetic parameter M on the velocity profiles in y direction $(g(\xi,\eta))$.

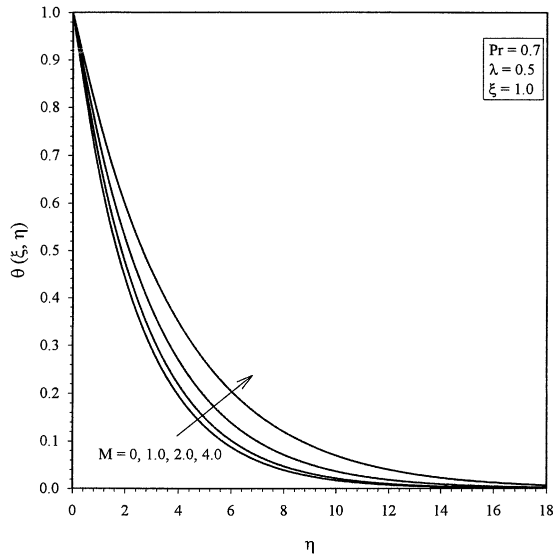

Fig. 10. Effect of the magnetic parameter M on the temperature profiles $(\theta(\xi,\eta))$.

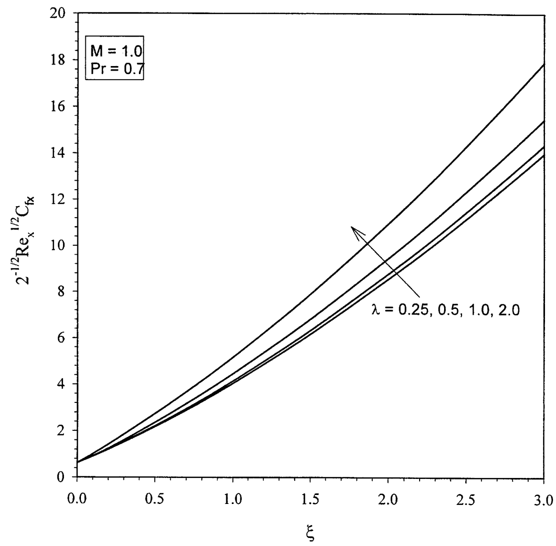

Fig. 11. Effect of the fluid rotation parameter λ on the local skin friction coefficient in x direction $(2^{-1/2}Re_x^{1/2}C_{fx})$.

duces the velocity in the y-direction $g(\xi,\eta)$ as is evident from Figs. 8 and 9. Consequently, the skin friction coefficient in x direction increases with M, but the skin friction coefficient in the y-direction decreases. Since the boundary-layer thickness decreases with increasing M, the velocity in the z-direction decreases with increasing M. This reduction in the velocity function f increases the thermal boundary layer thickness. Hence the Nusselt number decreases with increasing M. For $\xi = 3$, $\lambda = 0.5$, $Pr = 0.7$, the skin friction coefficient in the x-direction increases by about 96% as M increases from zero to 4, but the skin friction coefficient in the y-direction and the Nusselt number decrease, by about 57% and 30%, respectively.

The effect of the magnetic parameter M on the velocity and temperature profiles $(f'(\xi,\eta)$, $g(\xi,\eta)$, $\theta(\xi,\eta))$ for $\lambda = 0.5$, $\xi = 1$, $Pr = 0.7$ is given in Figs. 8–10. The velocity profiles in the x and y directions decrease with increasing M, but the temperature profiles are increased. This is due to the reduction of the momentum boundary layers and increase in the thermal boundary layer, with increasing M.

The effect of the fluid rotation, λ, on the skin friction coefficients and the Nusselt number $(2^{-1/2}Re_x^{1/2}C_{fx}$, $2^{-1/2}Re_x^{-1/2}$, C_{fy}, $2^{1/2}Re_x^{-1/2}Nu_x)$ for $M = 1$, $Pr = 0.7$ is presented in Figs. 11–13. Like M, λ is also multiplied by ξ. Hence the effect of λ vanishes at $\xi = 0$ and increases with ξ. Since the fluid rotation accelerates the fluid motion, the momentum boundary layer is reduced. Hence the skin friction coefficients are increased. Since the velocity in the z-direction f, is reduced due to the reduction in the bound-

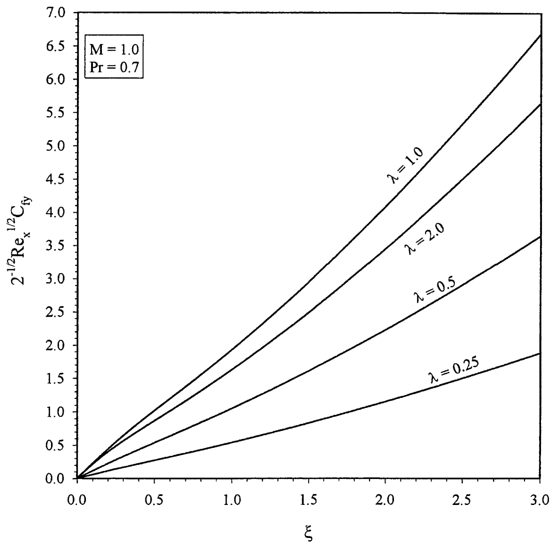

Fig. 12. Effect of the fluid rotation parameter λ on the local skin friction coefficient in y direction ($2^{-1/2}Re_x^{1/2}C_{fy}$).

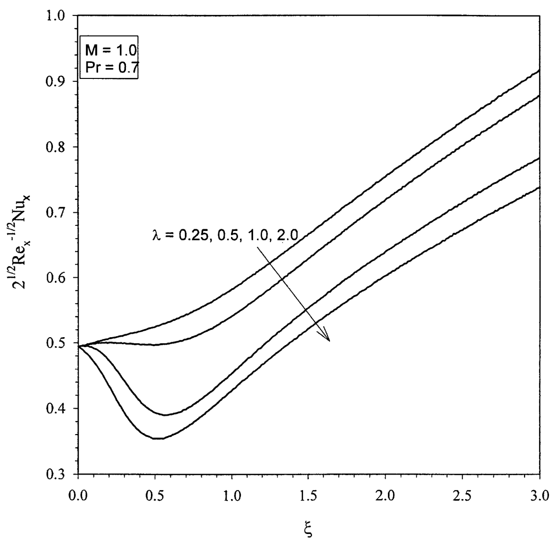

Fig. 13. Effect of the fluid rotation parameter λ on the local Nusselt number ($2^{1/2}Re_x^{-1/2}Nu_x$).

ary layer thickness, the Nusselt number is also reduced. For $\xi = 3$, $M = 1$, $Pr = 0.7$ the skin friction coefficients in the x and y directions increase by about 29% and 206%, as λ increases from 0.25 to 2 but the Nusselt number decreases by about 21%. The reason for the strong dependence of the skin friction in the y-direction on λ is that the secondary flow $g(\xi, \eta)$ is induced by λ ($g(\xi, \eta) = 0$ for $\lambda = 0$). It may be noted that the skin friction in the y-direction for $\lambda = 2$, is less than that for $\lambda = 1$. This trend is attributed to the compitition effects of various parameters. The effect of the Prandtl number Pr on the Nusselt number ($2^{1/2}Re_x^{-1/2}Nu_x$) for $M = 1$, $\lambda = 0.5$, is displayed in Fig. 14. Since the Prandtl number reduces the thermal boundary layer significantly, there is a considerable increase in the heat transfer rate with increasing

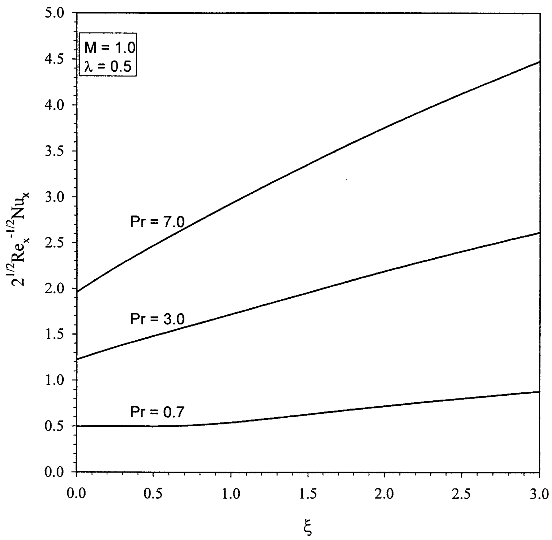

Fig. 14. Effect of the Prandtl number Pr on the local Nusselt number ($2^{1/2}Re_x^{-1/2}Nu_x$).

Pr. For $\xi = 3$, $M = 1$, $\lambda = 0.5$, the Nusselt number increase by about 430% as Pr increases from 0.7 to 7.

6. Conclusions

The Nusselt number is found to be strongly dependent on the Prandtl number and the suction (or injection) parameter. The skin friction coefficient in the case of primary flow is strongly affected by the magnetic field, whereas the skin friction coefficient for the secondary flow is strongly dependent on the rotation parameter. The velocity profiles in the primary and secondary flows are reduced by the magnetic field. The skin friction coefficients for both the primary and secondary flows, in general, increase significantly with the stream-wise distance. The results of the difference-differential method are in excellent agreement with those of the finite-difference method.

References

[1] B.C. Sakiadis, Boundary layer behaviour on continuous solid surface. II, The boundary layer on a continuos flat surface, Amer. Inst. Chem. Engrg. J. 7 (1961) 221–225.
[2] F.K. Tsou, E.M. Sparrow, R.J. Goldstein, Flow and heat transfer in the boundary layer on a continuously moving surface, Internat. J. Heat Mass Transfer 10 (1967) 219–235.
[3] E. Erickson, L.T. Fan, V.G. Fox, Heat and mass transfer on a moving continuous flat plate with suction or blowing, Indust. Engrg. Chem. Fund. 5 (1966) 19–25.
[4] J.F. Griffin, J.L. Throne, On the thermal boundary layer growth on continuous moving belts, Amer. Inst. Chem. Engrg. J. 13 (1967) 1210–1211.
[5] L.J. Crane, Flow past a stretching plate, Z. Angew. Math. Phys. 21 (1970) 445–447.
[6] P.S. Gupta, A.S. Gupta, Heat and mass transfer on a stretching sheet with suction or blowing, Canad. J. Chem. Engrg. 55 (1977) 744–746.

[7] A. Chakrabarti, A.S. Gupta, Hydromagnetic flow, heat and mass transfer over a stretching sheet, Quart. Appl. Math. 33 (1979) 73–78.

[8] P. Carragher, L.J. Crane, Heat transfer on a continuously moving sheet, Z. Angew. Math. Mech. 62 (1982) 564–565.

[9] B.K. Dutta, P. Roy, A.S. Gupta, Temperature field in flow over a stretching sheet with uniform heat flux, Internat. Comm. Heat Mass Transfer 28 (1985) 1234–1237.

[10] L.J. Grubka, K.M. Bobba, Heat transfer characteristics of a continuous stretching surface with variable temperature, J. Heat Transfer 107 (1985) 248–250.

[11] B.K. Dutta, Heat transfer from a stretching sheet with uniform suction or blowing, Acta Mech. 78 (1989) 255–262.

[12] P.R. Chappadi, P.S. Gunnerson, Analysis of heat and momentum transport along a moving surface, Internat. J. Heat Mass Transfer 32 (1989) 1383–1386.

[13] H.I. Andersson, An exact solution of the Navier–Stokes equations for MHD flow, Acta Mech. 113 (1995) 241–244.

[14] T.C. Chiam, Heat transfer with variable conductivity in a stagnation point flow towards a stretching sheet, Internat. Comm. Heat Mass Transfer 23 (1966) 239–248.

[15] K. Vajravelu, A. Hadjinicolaou, Convective heat transfer in an electrically conducting fluid at a stretching surface with uniform free stream, Internat. J. Engrg. Sci. 35 (1997) 1237–1244.

[16] M. Kumari, G. Nath, Flow and heat transfer in a stagnation point flow over a stretching sheet with a magnetic field, Mech. Res. Comm. 26 (1999) 469–478.

[17] D.R. Jeng, T.C.A. Chang, K.J. Dewitt, Momentum and heat transfer on a continuous moving surface, J. Heat Transfer 108 (1986) 532–537.

[18] C.Y. Wang, Stretching a surface in a rotating fluid, Z. Angew. Math. Phys. 39 (1988) 177–185.

[19] H.S. Takhar, G. Nath, Unsteady flow over a stretching surface with a magnetic filed in a rotating fluid, Z. Angew. Math. Phys. 49 (1998) 989–1001.

[20] R. Hide, P.H. Roberts, The origin of the mean geomagnetic field, in: Physics and Chemistry of the Earth, Vol. 4, Pergamon Press, New York, 1961, pp. 27–98.

[21] R.H. Dieke, Internal rotation of the sun, in: L. Goldberg (Ed.), Annual Review of Astronomy and Astrophysics, Vol. 8, Annual Review Inc, 1967, pp. 297–328.

[22] F.G. Blotnner, Finite-difference method of solution of the boundary layer equations, AIAA J. 8 (1970) 193–205.

[23] N.A. Jaffe, A.M.O. Smith, Calculation of laminar boundary layers by means of a differential-difference method, in: Progress in Aerospace Sciences, Pergamon Press, New York, 1972.

[24] A.C. Eringen, G.A. Maugin, Electrodynamics of Continua, Vol. 2, Springer-Verlag, Berlin, 1990.

[25] T.Y. Na, Computational Methods in Engineering Boundary Value Problems, Academic Press, New York, 1979.